SCIENTIFIC AND TECHNOLOGICAL RESEARCH ARTICLE

Analysis of wave climate and energy potential of intermediate waters in the marine sphere of influence of the main ports of the Colombian Caribbean

Análisis del clima marítimo de aguas intermedias y su potencial energético en la zona de influencia de los principales puertos del Caribe colombiano

DOI: https://doi.org/10.26640/22159045.2023.620 **Date received:** 2023-08-17 / Date accepted: 2023-11-10

Claudia Patricia Urbano-Latorre[1], Claudia Janeth Dagua Paz[2], Andrés Felipe Camilo Martínez[3]

CITATION:

Urbano-Latorre, C. P.; Dagua Paz, C. J.; Camilo Martínez, A. F. (2023). Analysis of wave climate and energy potential of intermediate waters in the marine sphere of influence of the main ports of the Colombian Caribbean. *CIOH Sci. Bull., 42*(2): 25-44. Online ISSN 2215-9045. DOI: https://doi.org/10.26640/22159045.2023.620

ABSTRACT

This paper presents a study of the wave climate of the Colombian Caribbean Sea, between coordinates 8° N and 16° N latitude and 84° W and 70° W longitude, and the energy potential at intermediate water points within the area of the Colombian Caribbean, which serve as inputs for the country's maritime interests. It was carried out based on the analysis of wave propagation simulations for 30 years developed at the Center for Oceanographic and Hydrographic Research of the Caribbean (CIOH), using the SWAN (Simulating WAves Nearshore) model, forced with the winds of the North American Regional Reanalysis (NARR) from 1979 to 2010 and validated with directional buoy data from the Colombian General Maritime Directorate (Dimar) and the United States National Oceanographic and Atmospheric Administration (NOAA) in the Caribbean. The results show four regions of similar wave height, period, and directional characteristics in the Colombian Caribbean. The first is the region around the islands of San Andrés and Providencia, and the second is a southern region between Urabá and Cartagena. A third comprises the central region around Barranquilla and Santa Marta, and the fourth, between Riohacha and Puerto Bolivar, occupies the northern part. The highest wave height values are observed for Barranquilla and Santa Marta, while the lowest are at Urabá. Furthermore, we evaluated the renewable wave energy capacity by studying the potential energy spectrum for virtual buoys in the primary ports. We observed that the energy was concentrated between 4 s and 6 s, with wave heights ranging from 0.5 m to 3 m for buoys in Barranquilla, Santa Marta, Puerto Bolivar, and Providencia. Amongst these, Barranquilla displayed the highest potential, with a period of 7 s and a wave height of 4m, followed by Santa Marta with values of 6 s and 3.8 m. The annual pattern of average energy potential revealed high values between December and March, medium values from June to August, and low values in May and between September and November; demonstrating that there is greater energy in the dry seasons and lower energy in the wet seasons. The wave conditions detected surpass the necessary threshold for energy generation via a Wave Energy Converter (WEC) alternative energy system, offering highly promising yield potentials, which could be magnified through the use of energy parks.

KEYWORDS: wave climatology, SWAN model, Colombian Caribbean Sea, wave potential energy

[1] Orcid: 0000-0002-2800-368X. Center for Oceanographic and Hydrographic Research of the Caribbean. "Almirante Padilla" Naval Cadet School, Isla de Manzanillo, barrio El Bosque, Colombia. Email: curbano@dimar.mil.co

[2] Orcid: 0000-0003-2865-6119 Center for Oceanographic and Hydrographic Research of the Caribbean. "Almirante Padilla" Naval Cadet School,Isla de Manzanillo, barrio El Bosque, Colombia. Email: claudia.dagua@gmail.com

[3] Orcid: 0009-0000-5507-7580. Center for Oceanographic and Hydrographic Research of the Caribbean. "Almirante Padilla" Naval Cadet School, Isla de Manzanillo, barrio El Bosque, Colombia. Email: acamilo@dimar.mil.co

Resumen

Este trabajo presenta un estudio del clima de oleaje para el mar Caribe colombiano, entre las coordenadas 8° N y 16° N de latitud y 84° W y 70° W de longitud, y su potencial energético en los puntos de aguas intermedias en el área de influencia marítima en los principales puertos del Caribe colombiano, que sirven de insumo a los intereses marítimos del país. Se realizó con base en análisis de simulaciones de propagación de oleaje de un período de 30 años elaborado en el Centro de Investigaciones Oceanográficas e Hidrográficas del Caribe, utilizando el modelo Simulating Wave Nearshore, forzado con los vientos del Reanálisis Regional de América del Norte de 1979 a 2010, y validado con información de boyas direccionales de la Dirección General Marítima y de la Administración Nacional Oceanográfica y Atmosférica en el mar Caribe. Los resultados muestran cuatro regiones del Caribe colombiano con características similares de altura, período y dirección de ola. La primera es la región insular de San Andrés y Providencia; la segunda, una región sur entre Urabá y Cartagena; una tercera es la región central, entre Barranquilla y Santa Marta; la cuarta corresponde a la parte norte, entre Riohacha y Puerto Bolívar. Los valores más altos de altura de ola se observan en Barranquilla y Santa Marta y los más bajos en Urabá. Adicionalmente, se evaluó la capacidad de energía renovable obtenida por medio del oleaje a partir del espectro de energía potencial para boyas virtuales en los principales puertos. Se encontró que la energía se concentra entre 4 s a 6 s de periodo, y entre 0.5 m y 3 m en alturas de ola, para las boyas de Barranquilla, Santa Marta, Puerto Bolívar y Providencia; siendo Barranquilla el sitio de mayor potencial que se encuentra entre 7 s y 4 m, seguida de Santa Marta entre 6 s y 3.8 m. El potencial energético promedio anual presenta valores altos entre diciembre y marzo; medios, entre junio y agosto; valores bajos, en mayo, y entre septiembre y noviembre, correspondientes a las épocas seca y húmeda. Las condiciones del oleaje encontradas superan el umbral necesario para generar energía con un sistema de energía alternativa tipo Wave Energy Converter, con potenciales de rendimiento aceptables que podrían multiplicarse mediante la instalación de parques energéticos.

Palabras clave: *climatología de olas, modelo SWAN, Caribe colombiano, potencial energético del oleaje.*

Introduction

The richness and diversity of marine energy resources in the Atlantic and Pacific basins are a privilege for Colombia, which has about 892 118 km2 of marine territory between the two basins (Invemar, 2015). Additionally, due to Colombia's subscription to different international maritime agreements, it is necessary to carry out maritime studies that provide knowledge of the territorial waters for purposes such as navigation, the exchange of goods, passenger transportation, vessel design and tourism, among others (Dimar, 2023).

Dimar, as Colombia's national maritime authority, has led oceanographic, meteorological and hydrographic studies that provide knowledge regarding the conditions of the seas and coasts under Colombian jurisdiction, through its marine scientific research centers located in the Caribbean and Colombian Pacific (González, 1987; Andrade, 1992; Molares, Vanegas, Bustamante & Andrade, 2004; Bastidas, 2011; Grisales, Salgado & Molares, 2014; Monroy & Zambrano, 2017; Casanova, Zambrano, Latandret, Guerrero, Suárez & Albán, 2019). To this end, different oceanographic campaigns and research projects have been carried out to contribute to the knowledge and understanding of the maritime dynamics of Colombia's territorial waters (Rueda, 2017; Dagua, Torres & Monroy, 2018; Moreno & Báez, 2021).

In 2006, Dimar began implementing a system for field monitoring of meteorological and oceanographic conditions along the Colombian coasts, with a project called Red de Medición de Parámetros Oceanográficos y de Meteorología Marina (RedMpomm), which includes meteorological stations, tide gauges and wave buoys on the Colombian Pacific and Caribbean coasts. This system offers support for maritime activities and provides information on in situ conditions in real time.

In addition to the information collected by Dimar, different authors have focused their attention on waves towards the construction,

expansion and adaptation of port structures which improve the flow of the maritime and river transport necessary for the coordination of logistics, using visual and instrumental data (Agudelo, Restrepo, Molares, Torres & Osorio, 2005), satellite databases (Thomas, Nicolae & Posada, 2012), as well as numerical modeling and reanalysis data (Mesa-García, 2009; Osorio, Mesa, Bernal & Montoya, 2009; Vega, Alvarez, Restrepo, Ortiz & Otero, 2020; Orejarena, Restrepo, Correa & Orfila, 2022).

Similarly, for more than a decade, specific studies evaluating wave energy potential have been carried out in Colombia. These have been performed at Isla Fuerte, located off the coast of Córdoba (Ortega, Osorio & Agudelo, 2013), the north of the peninsula of La Guajira, and Bocas de Ceniza in Barranquilla (Torres & Andrade, 2006), as well as for the entire Caribbean Sea, with special interest in the area of the Caribbean Low Level Jet (Appendini, Urbano, Figueroa, Dagua, Torres-Freyermuth, Salles, 2015). There studies have identified that, in the area including the Gulf of Mexico and the Caribbean Sea, the most energetic areas are found on the Colombian coastline.

Ocean energy has a key role to play in the sustainable development of coastal regions, as it can be integrated into local energy grids to supply, in addition to electricity, services such as water (from seawater desalination) and it can power electric transportation (Shadman *et al*., 2023). Colombia is advancing in an energy transition that will lead the country towards a green economy (DNP, 2023), supported by the National Development Plan (PND) 2023-2026 and the National Council for Bioceanic Economic and Social Policy (Conpes 3990) (DNP, 2020), which will contribute to the sustainable development of the country through the integrated and sustainable use of its strategic location, oceanic conditions and natural resources. Diversifying the country's energy matrix requires a broad knowledge of its resources. For this reason, and in order to study the maritime climate of the Colombian Caribbean and learn about its energy potential, in 2011 the Center for Oceanographic and Hydrographic Research of the Caribbean (CIOH) generated continuous synthetic wave time series, using a third generation numerical spectral wave model.

The hindcast employed made use of the SWAN (Simulating WAves Nearshore) model (Booji *et al*., 2004), which is based on the conservation of wave energy and winds from the North American Regional Reanalysis (NARR) project (Messinger, DiMego, Kalnay, Mitchell, Shafran & Ebisunaki 2006), from 1979 to 2010. The model was calibrated and validated using the data available from RedMpomm and it was verified that the model adequately reproduced the measurements (Dagua, Lonin, Urbano & Orfila, 2013). In this sense, this work aims to characterize the wave regime of the Colombian Caribbean based on the information generated, and calculate its energy potential. The work has been divided into sections on the maritime climate and energy potential; the former covers Colombia's jurisdictional waters in the Caribbean Sea and the latter uses specific points in the vicinity of the different harbor master's offices.

Study area

The Caribbean Sea begins at the Yucatan Peninsula and extends to Panama, bordered to the east by the Lesser Antilles and to the north by the Greater Antilles, ending at the island of Cuba. The predominant wind during most of the year comes from the east (known as trade winds) (Vernette, 1985; Nystuen & Andrade, 1993) and it is frequently affected by tropical waves, mainly between May and November (Sosa & Hernández, 2002). It is also affected by global-scale meteorological phenomena such as the North Atlantic Oscillation and the Southern Oscillation (Poveda, 1998; Amador, 2008).

There are two climatic seasons: a dry season between December and February, with higher wave heights, and a wet season between September and November, when wave height decreases. In addition, there is a transition period known as the Veranillo de San Juan (Bernal, Poveda, Roldán, Andrade, 2006) between June and August, with a peak wave height increase in July, after which it weakens until a low point in the wet season. The study area is located within Colombian jurisdictional waters in the Caribbean Sea, within which we selected the data point in intermediate waters ranging between 125 m and 250 m that is closest to the main ports of the Caribbean coast.

Methodology

In order to establish the characteristic parameters of waves and their effects in the region, it is essential to know their spatio-temporal evolution with sufficiently long time series, for which the CIOH's 30-year wave simulation database was chosen. Its domain in the Caribbean Sea is between latitudes 8° N and 18.7° N, and longitudes 84.5° W and 59.4° W (Fig. 1), with a spatial resolution of 12 km and a 1-hour temporal resolution. The output variables correspond to the integral wave parameters at each node: significant height (Hs), peak period (Tp) and predominant direction (Dir). The data were validated and calibrated with information measured by Dimar and National Oceanographic and Atmospheric Administration (NOAA) buoys, given that the numerically obtained data deviate from the instrumental data (Dagua *et al*., 2013), thus making it necessary to adjust the model parameterizations.

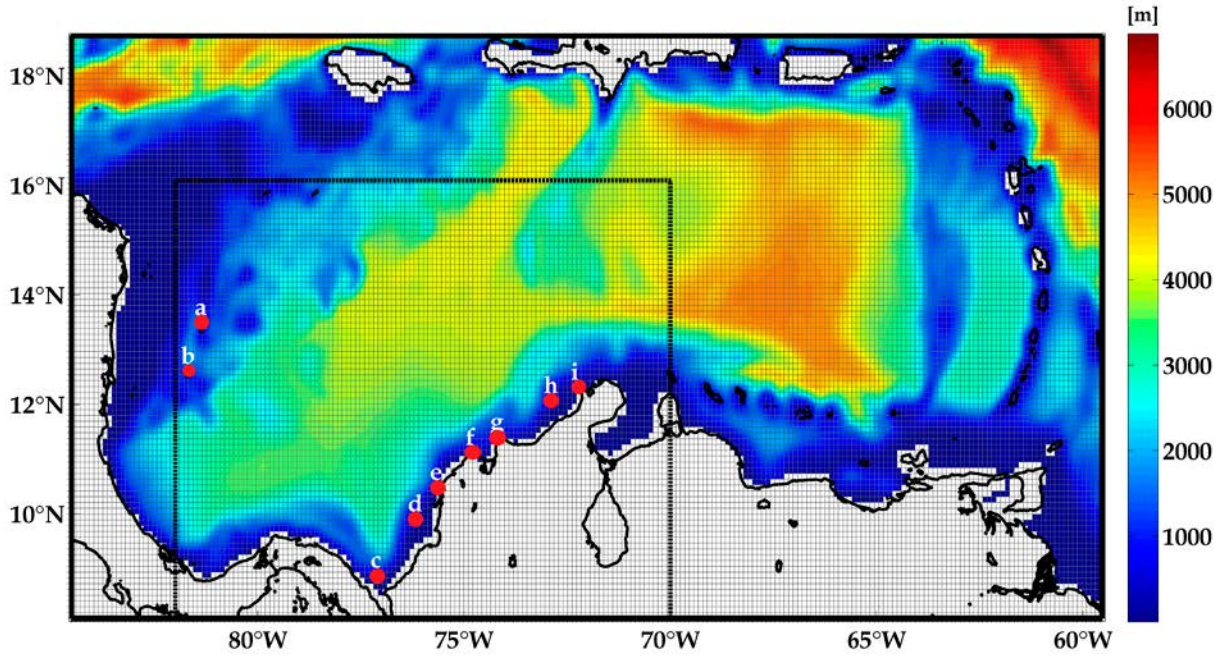

Figure 1. Computational domain of the wave modeling. The study area (--) with the location (red dots) of the virtual buoys: Providencia **(a)**, San Andrés Island **(b)**, Urabá **(c)**, Coveñas **(d)**, Cartagena **(e)**, Barranquilla **(f)**, Santa Marta **(g)**, Riohacha **(h)** and Puerto Bolívar **(i)**.

The data used to force the SWAN model were: bathymetry from ETOPO1 (Amante & Eakins, 2009) and winds from the NARR reanalysis (1979-2010), obtained from the Eta model of the US National Center of Environmental Prediction (NCEP); we used the zonal and meridional components of the wind at 10 m height, with a time step every three hours and a spatial resolution of 32 km.

For the analysis of the marine climate, a subdomain focused on Colombian jurisdictional waters was selected (Fig. 1, dotted line) between latitudes 8° N and 16° N, and longitudes 84° W and 70° W, and nine nodes were selected as virtual buoys located within 80 km of the main Colombian ports (Table 1).

Table 1. Coordinates of the virtual buoys from the SWAN model.

ID.	Region	Latitude (° N)	Longitude (° W)	Depth (m)
a	Providencia	13°31.98′	81° 19.98′	125
b	San Andrés	12° 38.82′	81° 40.38′	500
c	Urabá	08° 55.44′	77° 03.60′	250
d	Coveñas	09° 56.76′	76° 10.14′	250
e	Cartagena	10° 31.38′	75° 37.68′	250
f	Barranquilla	11° 09.66′	74° 45.60′	125
g	Santa Marta	11° 26.58′	74° 10.08′	250
h	Riohacha	12° 06.30′	72° 52.26′	250
i	Puerto Bolívar	12° 21.06′	72° 13.08′	125

Wave climate

Mean and extreme conditions of the sea state variables were calculated via a statistical analysis of the integral parameters for the study region. Mean conditions were obtained with the time average of each Hs and Tp series for all nodes in the study region. The probability of the joint density function was estimated using histograms of height and period in specific directions, providing monthly information on the propagation values for each wave period in a given direction.

For the extreme regime, although there is no single criterion to determine the wave conditions, it has been observed that distributions that consider two or three parameters are more appropriate (Ruiz *et al*., 2009). The distribution used corresponds to the Peaks Over Threshold (POT) method, following the methodology of Cañelas, Orfila, Méndez, Gómez-Pujol and Tintoré (2007). At the sites associated with the virtual buoys near the harbor master's offices, wave roses were produced to provide the predominant direction and associated wave height.

Calculation of power potential

To calculate the power potential using the integral wave parameters, an adjustment was made over the period (Booji *et al*., 2004) modeled in the 30-year historical wave analysis, which corresponds to:

$$T_{m,p-1,p} = 2\pi \frac{\iint \omega^{p-1} E(\omega,\theta) d\omega d\theta}{\iint \omega^{p} E(\omega,\theta) d\omega d\theta} \quad \textbf{(Eq.1)}$$

Where

$p = 0.5$ and $E = (\omega, \theta)$	Is the variation of the spectral power density.
ω	Is the absolute frequency determined by the change in the dispersion relation, bearing in mind the Doppler Effect and the wave direction .

Since the power flux P is a function of the significant wave height H_s (Vicinanza, Constetabile & Ferrante, 2013; Akpinar & Kömürcü, 2012; Rusu & Guedes, 2012; Aydogan, Ayat & Yüksel, 2013), the significance of the energy period is associated with a sine wave with the same energy as the sea state. For this reason, the energy period is the period parameter used to estimate wave energy in deep water:

$$P = \frac{\rho g^2 H_s^2 T_e}{64\pi} \quad \textbf{(Eq.2)}$$

Where,

ρ	is the density of seawater.

Meanwhile, in the SWAN model (Booji *et al*., 2004) T_e corresponds to another definition of the wave period, in the sense of the weighting factor for the spectral power in phase space:

$$RT_{m-10} = 2\pi \frac{\iint \sigma^{-1} E(\sigma,\theta) d\sigma d\theta}{\iint E(\sigma,\theta) d\sigma d\theta} \quad \textbf{(Eq.3)}$$

Where,

$E = (\sigma, \theta)$	is the spectral energy density.
σ	is the relative frequency of the wave and the wave direction θ.

Based on the methodology described by (Cahill & Lewis, 2014), which estimate the relationship between T_e and the zero-crossing period T_{02} for a Bretschneider and JONSWAP spectrum; the latter more adequately represents the waves in the Caribbean with a constant α (Torres & Lonin, 2007).

$$T_e = \alpha T_{02} \quad \textbf{(Eq.4)}$$

According to the spectral moments, Equation 4 can be written as:

$$\frac{m_{-1}}{m_0} = \alpha \sqrt{\frac{m_0}{m_2}} \quad \textbf{(Eq.5)}$$

By rearranging this equation in terms of H_{m0}, peak frequency f_p and the peak shape parameter γ, making the respective substitutions and simplifications, it is possible to rewrite the term α in terms of γ:

$$\alpha = \left(\frac{4.2+\gamma}{5+\gamma}\right) \cdot \left(\frac{11+\gamma}{5+\gamma}\right)^{\frac{1}{2}} \quad \textbf{(Eq.6)}$$

The values of the constant can vary according to the peak fitting parameter of the spectrum, γ, as shown in Table 2.

Table 2. Wave period ratio for the JONSWAP spectrum (Cahill & Lewis, 2014).

α	γ
1	1.22
2	1.20
3.3	1.18
5	1.16
7	1.14
10	1.12

The sensitivity of α to the shape of the spectrum indicates that the relationship is transient and that the values can fluctuate significantly at a site, depending on the conditions and the composition of the wave spectra; therefore, the constant cannot be defined if it is not corroborated with local information and a sufficiently long data series.

To make the fit between T and T_e, the correlation between the two variables was calculated. For this purpose, a year of wave propagation was simulated, in which the model was configured to calculate the two variables. It is assumed that in a one-year period the correlation between these two variables is statistically representative for the climatological conditions of the Caribbean.

For the simulated year, the time series was extracted for a node located east of Bocas de Ceniza, which is a zone with strong waves (-74.76° W and 11.16° N), and the respective correlation was made (Fig. 2) between the variables T and T_e.

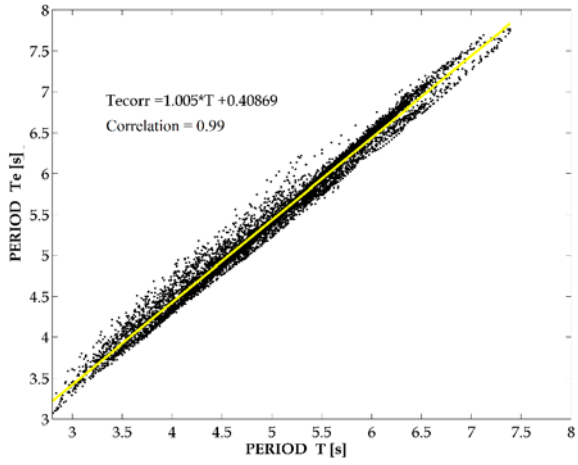

Figure 2. Correlation between the modeled variables T and T_e

The correlation coefficient is 0.99; however, was adjusted using the following equation obtained from the line of best fit, where is the calculated energy period:

$$T_{ec} = 1.005 * T + 0.4087 \quad \textbf{(Eq.7)}$$

The period T_{ec} was replaced and calculated. This adjustment was applied to the energy period for the nine virtual buoys and it was replaced in Equation 2 to obtain the power potential. The value of the constant used to adjust the period, α, is underestimated compared to the calculations presented in Table 2. This is because the period equation for performing the calculations by Cahill and Lewis (2014) is the zero crossing period, different from the average absolute period used for this case in the SWAN model.

Wave energy converter systems

The points in Table 1 were used to select a device to capture the wave energy of the Colombian Caribbean in the area of influence of the ports. Because depths range from 125 m to 250 m, the technology that can be used is the so-called offshore system (mounted at depths greater than 40 m) (Rodríguez-Abal, 2019; Pozos, 2019) or it is possible to explore a combination with nearshore technology (systems mounted at depths between 20 m and 30 m).

Next, we present some options of wave energy converter (WEC) devices that could be used to harness the energy, taking into account their power matrix (a diagram giving the power produced under certain wave conditions). This makes it possible to identify the maximum power generated by an instrument and to know its optimum performance:

- Pelamis: this device is versatile and can be adapted to a variety of depths (offshore wave energy harvesting system). It consists of a cylindrical structure, divided into several sections, that is located semi-submerged; its shape allows it to have two degrees of freedom, giving it horizontal and vertical mobility. The relative movement between the hinged parts pumps oil through a hydraulic system that feeds a pressurized cylinder which, in turn, drives an electricity generator and allows the capture of energy (Rodríguez-Abal, 2019; Vergaray, 2008). The orientation and shape allow power generation to be maximized when the waves are small. Table 3 presents the equipment's power matrix.

Table 3. Pelamis power matrix. Source: Rodríguez-Abal (2019).

Significant wave height (m) \ *Energy period (s)*	5	5.5	6	6.5	7	7.5	8	8.5	9	9.5	10	10.5	11	11.5	12	12.5	13
0.5	-	-	-	-	-	-	-	-	-		-	-	-	-	-	-	-
1	-	22	29	34	37	38	38	37	35	32	39	26	23	21	-	-	-
1.5	32	50	65	76	83	86	86	83	78	72	65	59	53	47	42	37	33
2	57	88	115	136	148	153	152	147	138	127	116	104	93	83	74	66	59
2.5	89	138	180	212	231	238	238	230	216	199	181	163	146	130	116	103	92
3	129	198	260	305	332	340	332	315	292	266	240	219	210	188	167	149	132
3.5	-	270	254	415	438	440	424	404	377	362	326	292	260	230	215	202	180
4	-	-	465	502	540	546	530	499	475	429	384	366	339	301	267	237	213
4.5	-	-	544	635	642	648	628	590	582	528	473	432	382	356	338	300	266
5	-	-	-	739	726	731	707	687	670	607	557	521	472	417	369	348	328
5.5	-	-	-	750	750	750	750	750	737	667	658	586	530	496	446	395	355
6	-	-	-	-	750	750	750	750	750	750	711	633	619	558	512	470	415
6.5	-	-	-	-	750	750	750	750	750	750	750	743	658	621	579	512	481
7	-	-	-	-	-	750	750	750	750	750	750	750	750	676	613	584	525
7.5	-	-	-	-	-	-	750	750	750	750	750	750	750	750	686	622	593
8	-	-	-	-	-	-	-	750	750	750	750	750	750	750	750	690	625

- OSWEC (nearshore wave energy capture system): This device is anchored to the seabed, therefore, its depth cannot exceed 30 m and it is located at a distance of 1 km from the coast (Morales, 2016). The system consists of a main paddle that receives the impact of the waves, and its dimensions depend on the bathymetry of the area where the equipment is installed. The paddle is mounted on a pivot which allows rotational movement induced by the interaction with the waves, using the power to drive a set of pistons that deliver pressurized water to the energy transformer unit. Table 4 presents the device's power matrix.

Table 4. OSWEC power matrix (OYSTER 800). Source: Rodríguez-Abal (2019).

Significant wave height (m) \ *Energy period (s)*	4	5	6	7	8	9	10	11	12	13	14	15	16
1	27	39	57	76	87	104	109	100	101	92	94	94	87
1.5	63	92	126	168	201	213	201	239	207	198	183	150	154
2	75	160	233	301	380	408	383	399	239	365	319	265	259
2.5	-	254	378	467	568	623	616	601	519	523	481	390	428
3	-	368	503	693	799	824	876	792	759	704	546	579	554
3.5	-	-	655	934	1032	1085	1241	1075	973	925	862	747	688
4	-	-	843	1093	1352	1427	1430	1390	1158	1224	1139	1138	863
4.5	-	-	1219	1408	1644	1677	1807	1641	1662	1562	1404	1370	1191
5	-	-	1247	1670	1965	1952	2097	2002	1833	1798	1814	1459	1442
5.5	-	-	-	1979	2339	2308	2115	2389	2120	2012	1940	1518	1587
6	-	-	-	2406	2713	2776	2344	2705	2451	2396	2182	2414	2133
6.5	-	-	-	2778	3044	3001	2989	3211	2986	2896	2716	2455	2309
7	-	-	-	2871	3119	3131	3127	3176	3332	2877	2925	2676	2658

Therefore, if we want to know the amount of power that can be generated with WEC (Wave Energy Converter) systems, it is necessary to correctly define the energy period and significant wave height in order to use the power matrix of the instrument. The power matrix defines the threshold value to activate the system and, in turn, gives the effective power for the wave characteristics.

The performance of the device is measured by the plant factor, which corresponds to the ratio between the effective power and the nominal power of the equipment. With this ratio, it is possible to know the percentage of the maximum possible power delivered by a WEC.

Plant factor = (effective power generated) / (nominal power) ×100 **(Ec.8)**

Results and discussion

From the calculation of the average deep water wave regime for the Colombian Caribbean Sea (Fig. 3a), it is evident how the waves are directly influenced by the wind (Fig. 3c), where the pattern of the wave and wind maxima are concentrated around the 75° W meridian with 12° N, north of the Colombian coasts, as a result of the Caribbean Low Level Jet, in agreement with what has been presented by other authors (Appendini *et al*., 2015; Wang & Lee, 2007). The maximum values for average Hs oscillate around 2 m, with wind speeds of 8 m/s.

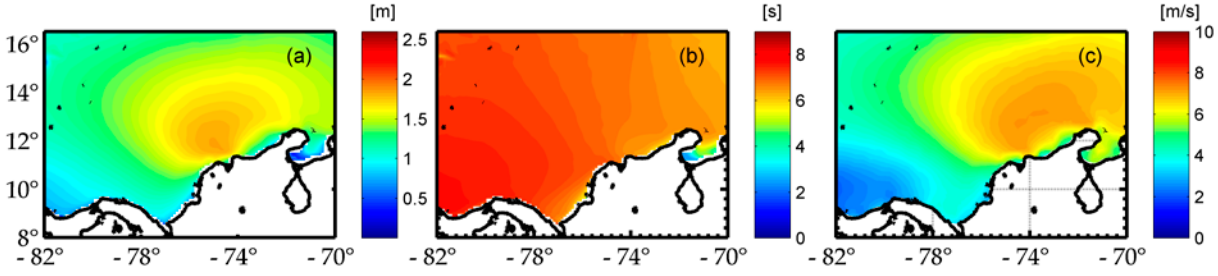

Figure 3. Mean values calculated from the 30-year database of CIOH reanalysis data: significant wave height **(a)**, peak period **(b)** and NARR reanalysis wind speed **(c)**.

The behavior of the peak period (Fig. 3b) is characterized by an east-west increase associated with the fetch, ranging from 6 s to 8 s. Although the winds over the Caribbean are not uniform (Fig. 3c), the wind sea waves increase their period depending on the fetch.

From Figure 3c, the values of moderate winds of U = 4 m/s (outside the La Guajira maximum) were used in the formula of Van Rijn (1994). The peak period is defined as $Tp = 0.286F^{*0.33}U/g$, where g is gravity and F* is the dimensionless fetch ($=gF/U^2$). It is calculated from this equation that a fetch of 546 km is required to reach the peak periods of 8 s (Fig. 3b). This coincides with the distance between the maximum winds (greater than 4 m/s) and the isthmus of Panama. It is important to mention that the wave height also depends on the fetch, but for the area of maximum wind the distribution of wind sea waves depends more on their intensity (Figures 3a and 3c).

Wave Climate in the Colombian Caribbean

The average regime allows us to characterize the wave behavior that will affect the coast on average. Figure 4 shows the average behavior of the significant wave height for each month of the year. This information is indispensable for studies for maritime works, bearing in mind that for a site near the coast it is necessary to propagate the deep water waves up to the point of interest.

From Figure 4, it can be observed that the wave behavior in the study area is, throughout the year, strongly influenced by the Caribbean Low Level Jet and the Intertropical Convergence Zone (ITCZ). Thus, during the months of December to March, during the dry season, the ITCZ is located further south, the trade winds are more intense, and the wave height is greater compared to the rest of the year.

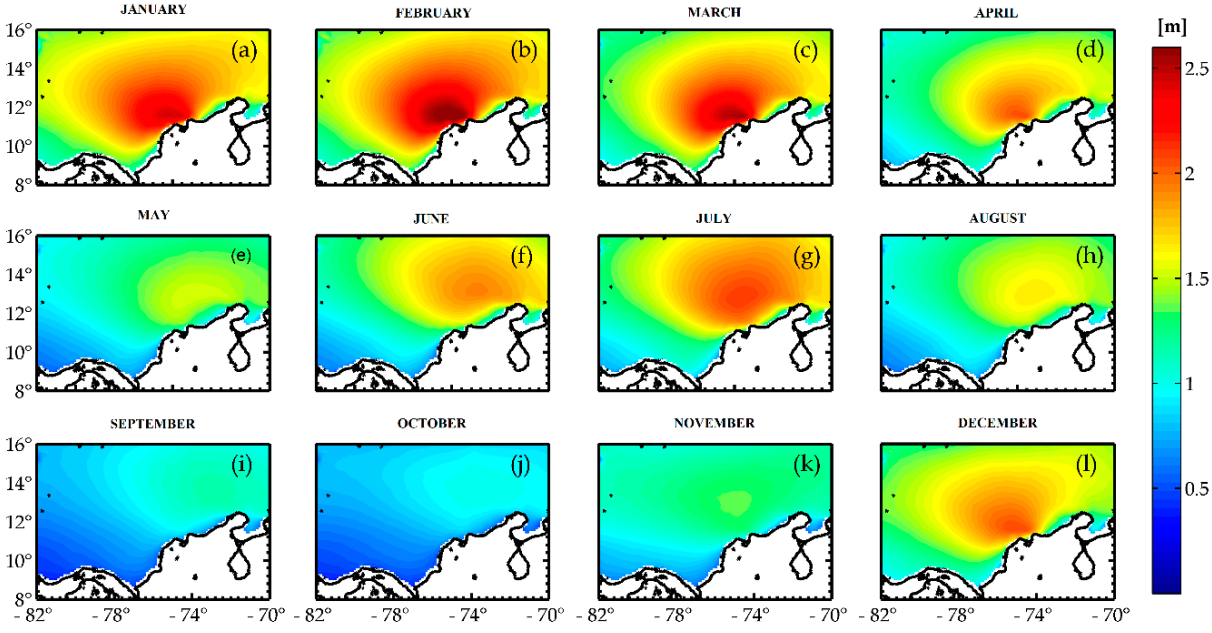

Figure 4. Monthly averages for significant wave height, based on the reanalysis information generated by the CIOH.

The opposite occurs during the months of September to November, which is the wet season and when the ITCZ is further north (Pujos & Mesa, 1988; Mesa, Poveda & Carvajal, 1997; Bernal *et al*., 2006). Likewise, Figure 4g (July) shows the influence of the San Juan dry season, with an increase in wave height compared to June and August (Figures 4f and 4h).

These results agree with those presented by Mesa-García (2009), who states that, in addition to spatial variability, the waves in the region have a temporal variation that manifests in the variability in the magnitude of the significant wave height in the different periods of the year.

In order to know in detail the wave behavior and its predominant direction in the vicinity of the main ports of the country, wave roses were produced for the locations of the virtual buoys given in Table 1 (Fig. 5).

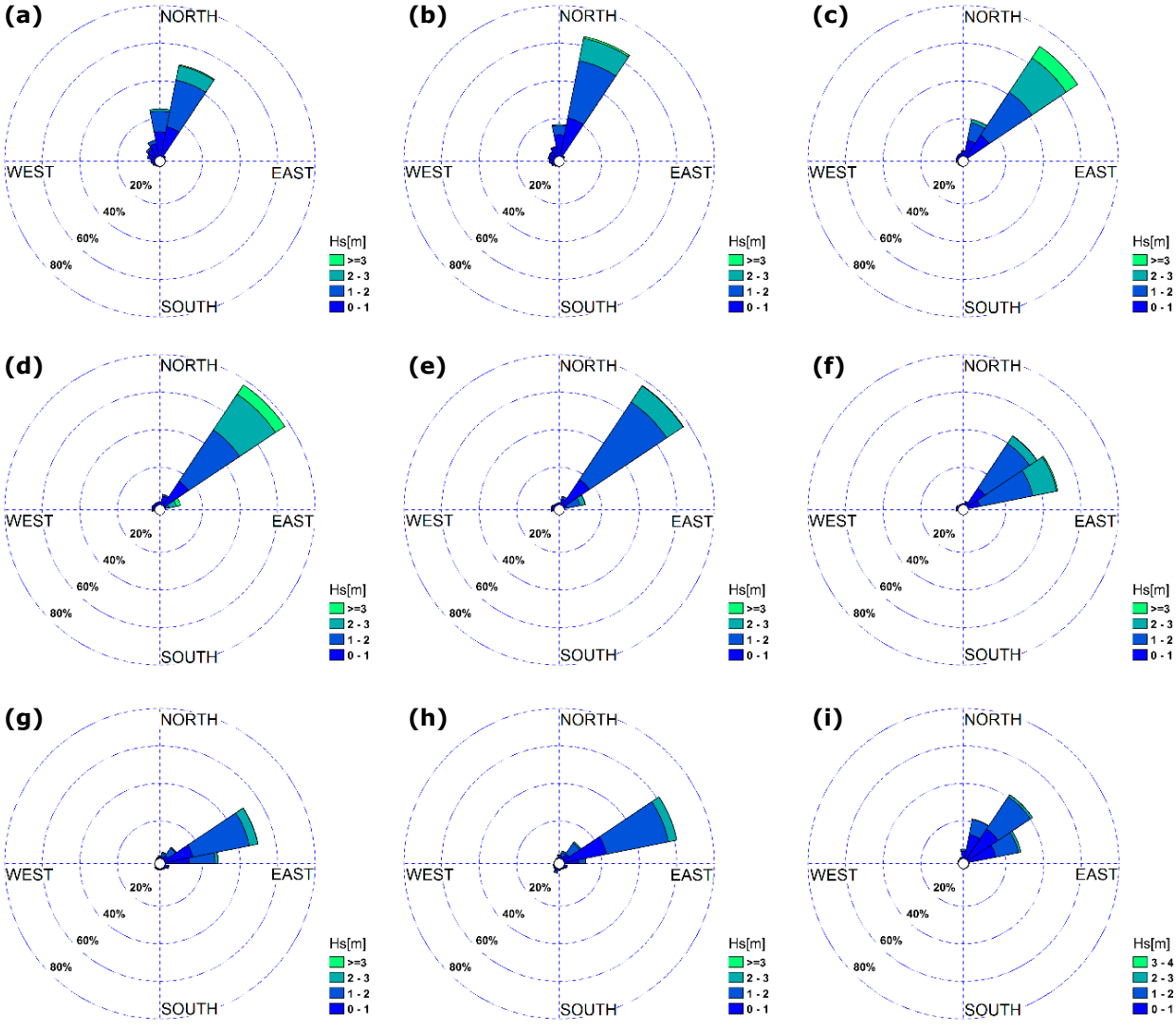

Figure 5. Wave roses for the study points, with associated wave height (color indicates Hs magnitude). Providencia **(a)**, San Andrés **(b)**, Urabá **(c)**, Coveñas **(d)**, Cartagena **(e)**, Barranquilla **(f)**, Santa Marta **(g)**, Riohacha **(h)**, Puerto Bolívar **(i)**.

For all the cases studied, it can be observed that wave directions are predominantly in the northeast (NE) quadrant. This behavior agrees with the wind climatology for the Caribbean described in (Vernette, 1985; Nystuen & Andrade, 1993), confirming a clear influence of the trade winds in the region.

The basic parameters of each virtual buoy are presented in Table 5, which shows the predominant direction and the proportion of time in which it occurs, as well as the significant wave height that is not exceeded 50% and 99% of the time for each location. It is observed that, for both the 50% and 99% occurrences, the maximum wave height value is for Barranquilla and the lowest is for Urabá, something which is corroborated both in the calculated mean regime (Fig. 3) and in the monthly averages (Fig. 4).

Table 5. Description of the predominant direction and wave height for each virtual buoy.

Virtual buoy	Direction	Direction Probability (%)	Hs50%	Hs99%
Providencia	NEE	50.60	1.275	2.613
San Andrés	NEE	61.24	1.174	2.542
Urabá	NE	41.45	1.047	2.290
Coveñas	NNE	49.63	1.311	3.044
Cartagena	NNE	64.82	1.338	3.104
Barranquilla	NE	70.69	1.777	3.953
Santa Marta	NE	77.32	1.700	3.770
Riohacha	NE	76.92	1.419	2.754
Pto. Bolívar	NEE	48.77	1.677	3.067

Figure 6 shows the results of the extreme regime, with different return periods.

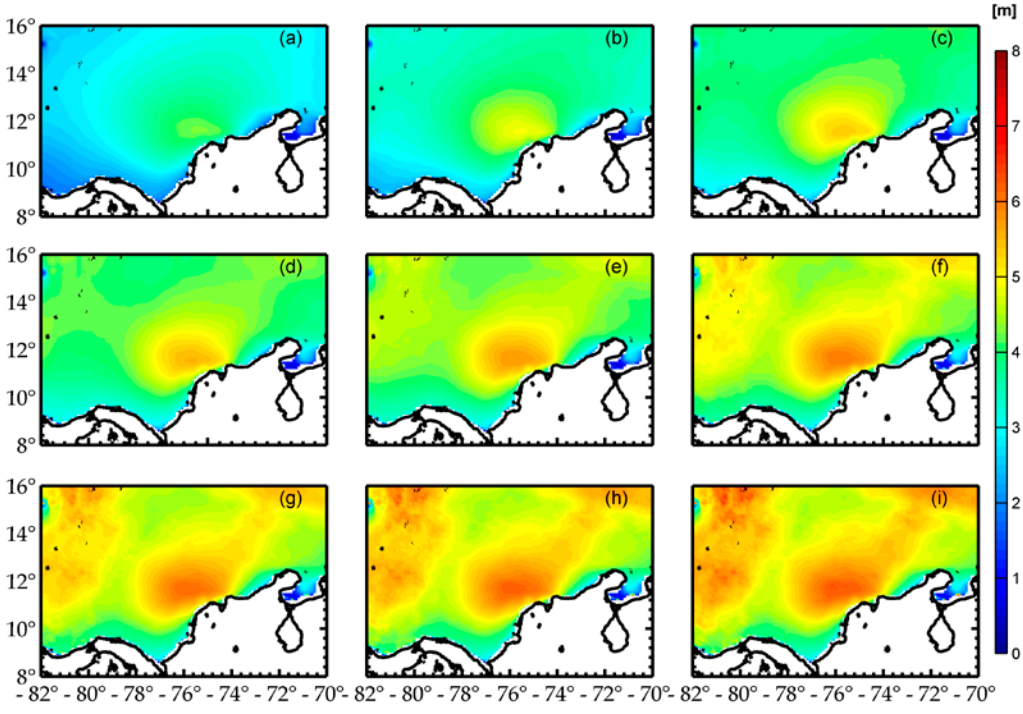

Figure 6. Extreme waves for deep water in the study area. Wave height for the 99% threshold **(a)**, 1-year return period **(b)**, 3-year return period **(c)**, 5-year return period **(d)**, 10-year return period **(e)**, 20-year return period **(f)**, 30-year return period **(g)**, 50-year return period **(h)**, 100-year return period **(i)**.

The waves associated with extreme events has their lowest heights in the Urabá region in the southernmost area of the Caribbean Sea, as well as in Coveñas, which, given its position, is less exposed to the strongest storms coming from the east. The regions of Providencia and San Andres have high wave values in the different return periods, but the highest extreme wave height values occur in deep waters in the regions of Barranquilla and Santa Marta, with associated wave heights of around 6 m.

Although the results presented in this study agree with the mean values of height and predominant direction presented by other authors (Agudelo *et al*., 2005; Osorio *et al*., 2009; Thomas, Nicolae, Durand, Posada, García & Andrade 2011), the extreme values differ for different return periods and regions. This is attributed to the fact that the databases used are different (data from traveling ships or satellite altimetry), as well as the methodologies used for their calculation (annual maximum, GEV, POT).

In this sense, it is clear that wave statistics (through wind reanalysis) should better reflect these values compared to the observations from traveling ships: (*i)* due to visual observation errors and subjective experiences; *(ii)* because they occur in different locations when there is a need to group the data in a grid; *(iii)* as ships avoid severe adverse phenomena, such as tropical cyclones, in the shipping lanes.

Potential of wave energy for points close to the harbor master's offices

The expressions for calculating power described in the methodology were used to obtain scatter and energy diagrams in terms of Hs and Te (Fig. 7). These describe the average power potential of a year, for intervals of 0.25 m and 0.25 s, respectively.

According to these results, the power potential is concentrated between 4 s and 6 s and between 0.5 m and 3 m, similar to the figures reported by Appendini *et al*. (2015) for the Barranquilla, Puerto Bolivar and Providencia buoys. The highest potential is observed for the Barranquilla buoy, at around 7 s and 4 m; followed by Santa Marta, around 6 s and 3.8 m, taking into account that the power lines vary according to the period and wave height.

It should be noted that the frequency of these values is low, considering that the color bar establishes the proportion of time (in hours) that a certain amount of megawatts is available or generated, calculated for an average year. Therefore, although Barranquilla's maximum potential is around 50 kW/m, these conditions will only generate less than 0.1 MWh per year. Finally, to establish the most favorable conditions of energy flow, the seasonal variability of the potential was calculated, giving averages over the year for each virtual buoy (Fig. 8).

In general, high values of power potential in the annual cycle are observed from December to March, in the dry season, and the lowest values in May and between September and November, months that correspond to the wet seasons, respectively (Bernal *et al*., 2006). But there is also an increase in July, related to the Veranillo de San Juan or transitional season (Andrade & Barton, 2000; Curtis & Gamble, 2007).

As in the potential energy diagrams, the virtual buoys of Barranquilla and Santa Marta have higher values than the other buoys. This is explained due to their geographical location close to the Caribbean Low Level Jet (Appendini *et al*., 2015; Ruiz & Bernal, 2009; Bernal, Ruiz & Beier, 2010; Andrade & Barton, 2005). This affects the waves as recorded in the pattern of the mean significant wave height value (Fig. 3) and confirmed in its monthly variability (Fig. 4).

Effective potential calculated for the points near the harbor master's offices

According to the study, the points with the greatest potential are located near Barranquilla and Santa Marta, where between 55 Kw/m and 43 Kw/m, respectively, could be obtained. However, this is not the real potential achieved with WEC systems.

Considering the wave characteristics of Figure 7, it is possible to define the Hs intervals and energy periods that are maintained throughout the year. With this information the real power (effective power) generated with the Pelamis and Oyster instruments, described earlier, was

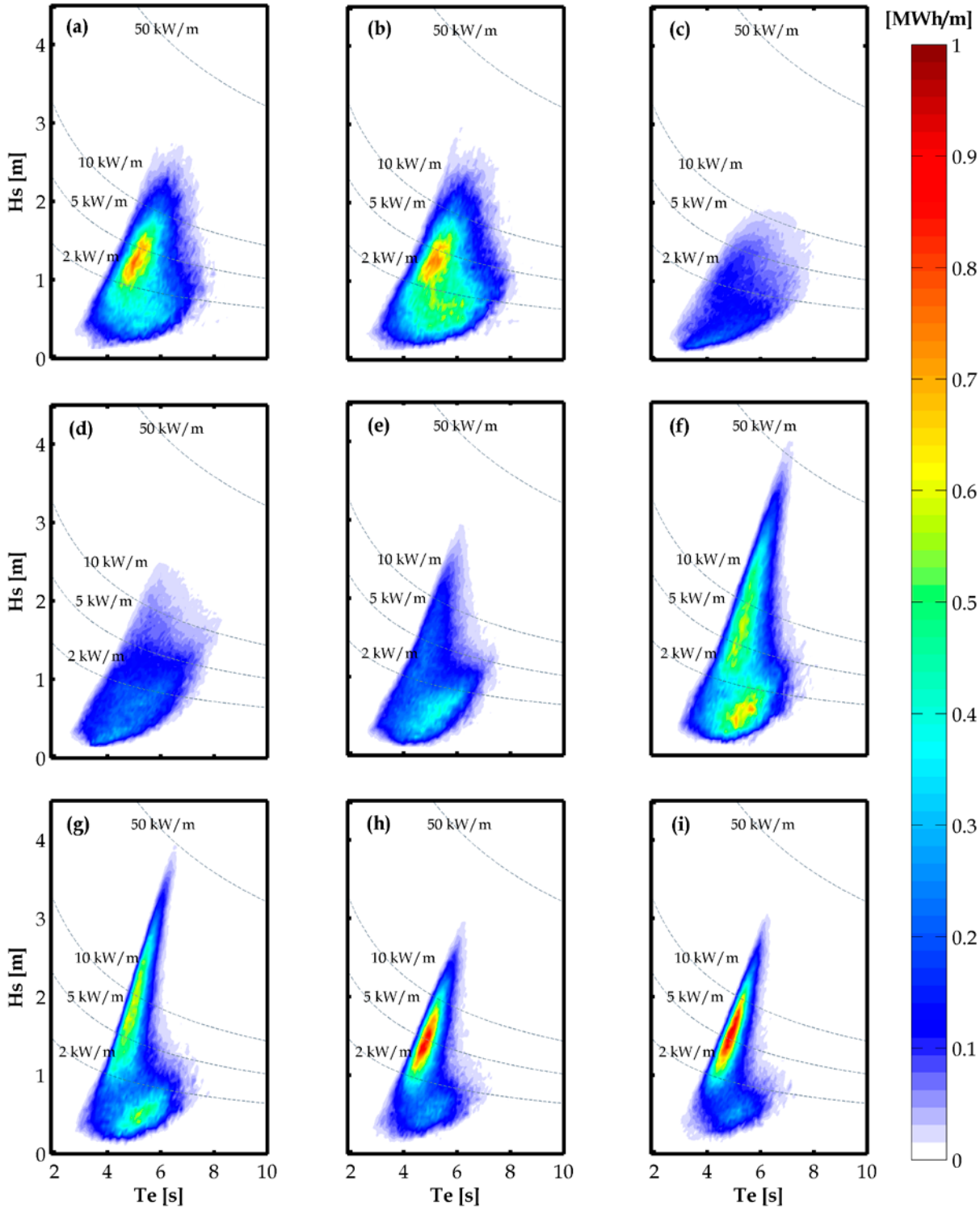

Figure 7. The combined scatter and energy diagrams of Hs and Te for the virtual buoys near: Providencia **(a)**, San Andrés **(b)**, Urabá **(c)**, Coveñas **(d)**, Cartagena **(e)**, Barranquilla **(f)**, Santa Marta **(g)**, Riohacha **(h)**, Puerto Bolívar **(i)**. The dotted line indicates the potential power (per meter of wave front) and the colors give the power per unit of time

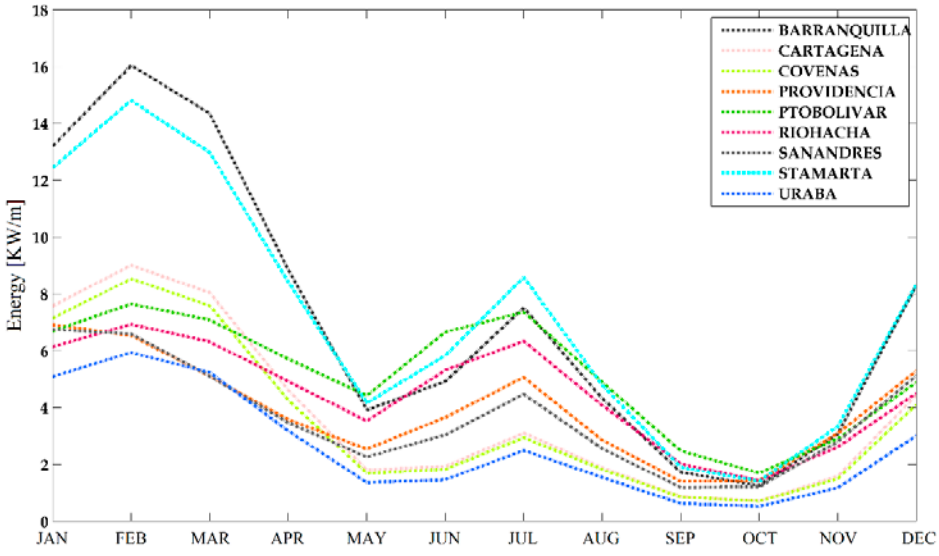

Figure 8. Average annual power potential for the virtual buoys near Providencia, San Andrés, Urabá, Coveñas, Cartagena, Barranquilla, Santa Marta, Riohacha and Puerto Bolívar.

calculated for each of the study areas. In addition to the real potential, it is possible to generate the plant factor and define the percentages of the energy that each instrument would capture (Eq. 8). Tables 6, 7, 8 and 9 present the performance of the Pelamis and Oyster instruments for the Barranquilla and Santa Marta areas, in which the color variations (gray-lower to red-higher) reflect the power and yield of each of the devices considered, depending on the wave conditions.

Table 6. Power matrix and plant factor for Barranquilla with Pelamis technology

		Power Generation Matrix for Barranquilla							
		Period (s)							
		4	4.5	5	5.5	6	6.5	7	7.5
Hs (m)	0.5	-	-	-	-	-	-	-	-
	1	-	-	-	22	29	34	37	38
	1.5	-	-	32	50	65	76	83	86
	2	-	-	57	88	115	136	148	153
	2.5	-	-	89	138	180	212	231	238
	3	-	-	129	198	260	305	332	340
	3.5	-	-	-	270	254	415	438	440
	4	-	-	-	-	465	502	540	546
		Plant Factor for Barranquilla							
		Period (s)							
		4	4.5	5	5.5	6	6.5	7	7.5
Hs (m)	0.5	-	-	-	-	-	-	-	-
	1	-	-	-	3 %	4 %	5 %	5 %	5 %
	1.5	-	-	4 %	7 %	9 %	10 %	11 %	11 %
	2	-	-	8 %	12 %	15 %	18 %	20 %	20 %
	2.5	-	-	12 %	18 %	24 %	28 %	31 %	32 %
	3	-	-	17 %	26 %	35 %	41 %	44 %	45 %
	3.5	-	-	-	36 %	34 %	55 %	58 %	59 %
	4	-	-	-	-	62 %	67 %	72 %	73 %

Table 7. Power matrix and plant factor for Santa Marta with Pelamis technology

		Power Generation Matrix for Santa Marta					
		Period (s)					
		4	4.5	5	5.5	6	6.5
Hs (m)	0.5	-	-	-	-	-	-
	1	-	-	-	22	29	34
	1.5	-	-	32	50	65	76
	2	-	-	57	88	115	136
	2.5	-	-	89	138	180	212
	3	-	-	129	198	260	305
	3.5	-	-	-	270	254	415
	4	-	-	-	-	465	502
		Plant Factor for Santa Marta					
		Period (s)					
		4	4.5	5	5.5	6	6.5
Hs (m)	0.5	-	-	-	-	-	-
	1	-	-	-	3 %	4 %	5 %
	1.5	-	-	4 %	7 %	9 %	10 %
	2	-	-	8 %	12 %	15 %	18 %
	2.5	-	-	12 %	18 %	24 %	28 %
	3	-	-	17 %	26 %	35 %	41 %
	3.5	-	-	-	36 %	34 %	55 %
	4	-	-	-	-	62 %	67 %

Tabla 8. Power matrix and plant factor for Barranquilla with Oyster technology

		Power Generation Matrix for Barranquilla			
		Period (s)			
		4	5	6	7
Hs (m)	0.5	-	-	-	-
	1	27	39	57	76
	1.5	63	92	126	168
	2	75	160	233	301
	2.5	-	254	378	465
	3	-	368	503	693
	3.5	-	-	655	934
	4	-	-	843	1093
		Plant Factor for Barranquilla			
		Period (s)			
		4	5	6	7
Hs (m)	0.5	-	-	-	-
	1	1 %	1 %	2 %	2 %
	1.5	2 %	3 %	4 %	5 %
	2	2 %	5 %	7 %	9 %
	2.5	-	8 %	11 %	14 %
	3	-	11 %	15 %	21 %
	3.5	-	-	20 %	28 %
	4	-	-	25 %	33 %

Tabla 9. Power matrix and plant factor for Santa Marta with Oyster technology

		Power Generation Matrix for Santa Marta		
		Period (s)		
Hs (m)		4	5	6
	0.5	-	-	-
	1	27	39	57
	1.5	63	92	126
	2	75	160	233
	2.5	-	254	378
	3	-	368	503
	3.5	-	-	655
	4	-	-	843
		Plant Factor for Santa Marta		
		Period (s)		
Hs (m)		4	5	6
	0.5	-	-	-
	1	1 %	1 %	2%
	1.5	2 %	3 %	4 %
	2	2 %	5 %	7 %
	2.5	-	8 %	11 %
	3	-	11 %	15 %
	3.5	-	-	20 %
	4	-	-	25 %

In Barranquilla and Santa Marta, 546 Kw/m and 502 Kw/m respectively can be achieved with a Pelamis WEC, which represents an efficiency of 73% and 67%, in maximum wave conditions. However, these conditions are not constant over time, as shown in Figure 7. Potentials between 115 Kw/m and 88 Kw/m would be obtained with greater frequency, representing an efficiency of 15 % and 12 %. The variability of the conditions means that the system does not maintain maximum generation; therefore, conditions should be sought in which an almost constant electrical generation is achieved as recommended by (Rodriguez-Abal, 2019), thereby achieving a reliable system which generates the power necessary to meet the demand of users.

With an Oyster device, under maximum wave conditions, electricity potentials of 1 093 Kw/m and 843 Kw/m are achieved for Barranquilla and Santa Marta respectively, which reflects plant factors of 33% and 25%. However, as previously mentioned, these conditions are not constant over time. Potentials of 233 Kw/m and 160 Kw/m would be obtained with greater frequency, which indicate a yield of 7% and 5% at the two ports. Compared to a Pelamis system, the Oyster delivers higher electrical potentials, but the performance of the equipment does not reach the percentages shown by Pelamis as a consequence of its higher nominal power.

Conclusions

Four regions of similar wave height, period and direction characteristics were identified in the Colombian Caribbean. The first is an insular region corresponding to San Andrés and Providencia; there is a southern region located between Urabá, Coveñas and Cartagena; a central region corresponds to the region around Barranquilla and Santa Marta; and a northern region is found between Riohacha and Puerto Bolívar.

The study shows that Barranquilla and Santa Marta have higher wave height values compared to the other regions, in both the 50% and 99% probability calculations, while the lowest values are found at Providencia, San Andrés and Urabá. For the case of extreme regimes, the highest extreme wave height values occur in deep waters in the regions of Barranquilla and Santa Marta, and the lowest in the regions of Urabá and Coveñas.

The spectrum of potential energy for the virtual buoys is concentrated between 4 s to 6 s in period and between 0.5 m and 3 m in wave height, very similar to that reported by (Appendini *et al*., 2015) for the buoys of Barranquilla, Puerto Bolivar and Providencia. The highest potential is observed at the Barranquilla buoy with 7 s and 4 m, followed by Santa Marta with 6 s and 3.8 m.

The annual average of potential energy has high values for the dry months of December to March, while it has low values in May, and between September and November, corresponding to the wet seasons. The statistics and databases produced in this work provide reference information on the process of wave transformation in transitory and shallow waters in the maritime zone of influence of all the port captaincies of the Caribbean.

In this sense, taking into account that most of the research on wave energy in Colombia has focused on characterizing the resource by measuring the height and period of the waves, it is relevant to develop, optimize and characterize equipment to identify the feasibility of this type of technology, and develop devices for generating energy from the resources available in the country.

According to the results of this study, the wave conditions exceed the threshold necessary to activate a WEC system, with possibly acceptable yield potentials, which could be multiplied when setting up energy parks involving more than one or two WEC devices and making a more exhaustive analysis of the topographic conditions of the installation areas. In the end, the viability of these systems will be subject to economic factors, which will mark the cost-benefit ratio of this type of emerging technology.

Funding Source

This work was produced using the resources of the Center for Oceanographic and Hydrographic Research of the Caribbean (CIOH), part of the General Maritime Directorate (Dimar).

Author contributions

Conceptualization, C. U.; methodology, C. U.; data curation: C. D., A. C.; analysis, C. U., C. D., A. C; software: C. U., C. D., A. C.; visualization, C. U.; writing – original draft preparation, C. U.; writing – review and editing, C. U., C. D. All the authors have read and accepted the published version of the manuscript.

References

Agudelo, P.; Restrepo, A.; Molares, R.; Torres, R.; Osorio, A. (2005). Determinación del clima de oleaje medio y extremal en el Caribe colombiano. *Bol. Cient. CIOH, 23: 33-45.* https://doi.org/10.26640/22159045.137

Akpinar, A.; Kömürcü, M. (2012). Wave energy potential along the south-east coast of the Black Sea. *Energy, 42(2): 289-302.* https://doi.org/10.1016/j.energy.2012.03.057

Amador, J. (2008). El jet de bajo nivel del mar Intraamericano. *Anales de la Academia de Ciencias de Nueva York, 1146: 153-188.* https://doi.org/10.1196/annals.1446.012 PMid:19076415

Amante, C.; Eakins, B. (2009). *ETOPO 1 1 arc-Minute Global Relief Model: Procedures, Data Sources and Analysis.* National Geophysical Data Center, Marine Geology and Geophysics Division. Boulder, Colorado: NOAA Tecnical Memorandum NESGIS NGDC-24.

Andrade, C. A. (1992). Movimiento geostrófico en el Pacífico colombiano*. Bol. Cient. CIOH, 12: 23-38.* https://doi.org/10.26640/01200542.12.23_38

Andrade, C. A.; Barton, E. (2000). Eddy development and motion in the Caribbean Sea. *Journal of Geophysical Research,* 105(C11): 26191-26201. https://doi.org/10.1029/2000JC000300

Andrade, C. A.; Barton, E. D. (2005). The Guajira upwelling system. *Continental Shelf Research,* 25(9): 1003-1022. https://doi.org/10.1016/j.csr.2004.12.012

Appendini, C.; Urbano, C.; Figueroa, B.; Dagua, C.; Torres-Freyermuth, A.; Salles, P. (2015). Wave energy potential assessment in the Caribbean Low Level Jet using. *Applied Energy,* 137: 375-384. https://doi.org/10.1016/j.apenergy.2014.10.038

Aydogan, B.; Ayat, B.; Yüksel, Y. (2013). Black Sea wave energy atlas from 13 years hindcasted

wave data. *Renewable Energy, 57: 436-447.* https://doi.org/10.1016/j.renene.2013.01.047

Bastidas, G. D. (2011). Evaluación temporal de parámetros fisicoquímicos en una estación oceánica frente a la bahía de Tumaco. *Bol. Cient. CIOH, 29: 137-145.* https://doi.org/10.26640/22159045.236

Bernal, G.; Poveda, G.; Roldán, P.; Andrade, C. (2006). Patrones de variabilidad de las temperaturas superficiales del mar en la costa Caribe colombiana. *Revista de la Academia Colombiana de Ciencias Exactas, Físicas y Naturales, 30(115): 195-208.*

Bernal, G.; Ruiz, M.; Beier, E. (2010). Variabilidad estacional e interanual océano-atmósfera en la cuenca Colombia. *Cuadernos del Caribe, 14: 49-72.*

Booji, N.; Haagsma, I.; Holthuijsen, L.; Kieftenburg, A.; Ris, R.; Van der Westhuysen, A., Zijlema, M. (2004). SWAN Usermanual, CycleIII Version 40.51. Netherlands: Delft University of Technology.

Cahill, B.; Lewis, T. (2014). *Wave period ratios and the calculation of wave power.* Seattle: Proceedings of the 2° Marine Energy Technology Symposium.

Cañelas, B.; Orfila, A.; Méndez, F.; Gómez-Pujol, L.; Tintoré, J. (2007). Application of a POT model to estimate the extreme significant wave height levels around the Balearic Sea (Western Mediterranean). *Journal of Costal Research, 50: 329-333.*

Casanova, R.; Zambrano, M.; Latandret, S.; Guerrero, D.; Suárez, N.; Albán, C. (2019). Comportamiento espacial de algunas variables fisicoquímicas en el Pacífico colombiano durante el Crucero Oceanográfico Cuenca Pacífica Colombiana CPC XLIX. Bol. Cient. CIOH, 38(1): 8-19. https://doi.org/10.26640/22159045.2019.520

Curtis, S.; Gamble, D. (2007). Regional variotions of the Caribbean mid-summer drought. *Theoretical and Applied Climatology,* 94: 25-34. https://doi:10.1007/s00704-007-0342-0

Dagua, C.; Torres, R.; Monroy, J. (2018). Condiciones oceanográficas de la reserva de biósfera Seaflower 2014–2016. *Bol. Cient. CIOH, 37: 53-74.* https://doi.org/10.26640/22159045.449

Dagua, C.; Lonin, S.; Urbano, C.; Orfila, A. (2013). Calibración del modelo SWAN y validación de reanálisis de oleaje en el Caribe. *Bol. Cient. CIOH, 31: 13-28.* https://doi.org/10.26640/22159045.249

Departamento Nacional de Planeación. (2020). *Documento CONPES 3990 "Colombia potencia bioceánica sostenible 2030". Bogotá. 91 pp.* https://colaboracion.dnp.gov.co/CDT/Conpes/Econ%C3%B3micos/3990.pdf

Departamento Nacional de Planeación. (2023). *Plan Nacional de Desarrollo 2023- 2026 "Colombia potencia mundial de la vida". Bogotá. 345 pp.* https://www.dnp.gov.co/plan-nacional-desarrollo/pnd-2022-2026

Dirección General Marítima. (2023). *Convenios OMI (Organización Marítima Internacional).* https://www.dimar.mil.co/Internacional/convenios-omi-organizacion-maritima-internacional-0

González, E. (1987). Oceanografía física descriptiva del archipiélago de San Andrés y Providencia, con base en el análisis de los cruceros Océano IV a IX. *Bol. Cient. CIOH, 7: 73-100.* https://doi.org/10.26640/01200542.7.73_100

Grisales, C.; Salgado, J.; Molares, R. (2014). Proceso de intercambio de masas de agua de la bahía de Cartagena (Caribe colombiano) basado en la medición de parámetros oceanográficos. *Bol. Cient. CIOH, 32: 47-70.* https://doi.org/10.26640/22159045.263

Instituto de Investigaciones Marinas y Costeras "José Benito Vives de Andréis". (Enero de 2015). *Noticias Invemar.* https://www.invemar.org.co/50-mar#:~:text=El%20%C3%A1rea%20terrestre%20es%20de,la%20cifra%20que%20se%20use)

Mesa-García, J. (2009). *Metodología para el reanálisis de series de oleaje para el Caribe Colombiano. Universidad Nacional de Colombia - Sede Medellín. Medellín, Colombia.*

Mesa, O.; Poveda, G.; Carvajal, L. (1997). Introducción al clima de Colombia. Universidad Nacional de Colombia. Medellín, Colombia.

Messinger, F.; DiMego, G.; Kalnay, E.; Mitchell, K.; Shafran, P.; Ebisunaki, W. (2006). North american regional reanalysis. *Bulletin American Meteorological Society*, 87: 343-360. https://doi.org/10.1175/BAMS-87-3-343

Molares, R.; Vanegas, T.; Bustamante, J.; Andrade, C. (2004). Aspectos oceanográficos de las aguas sobre la depresión Providencia en mayo de 2004. *Bol. Cient. CIOH, 22: 11-25.* https://doi.org/10.26640/22159045.124

Morales, E., (2016). *Análisis de un dispositivo oscilante como medio de captación de energía undimotriz. Tesis para optar a ingeniero civil mecánico. Universidad de Chile.* https://repositorio.uchile.cl/

Monroy, J.; Zambrano, A. (2017). Aspectos físicos del agua de mar entre las islas de Providencia y Cayo Bajo Nuevo durante la época de lluvias de 2016. *Bol. Cient. CIOH, 35: 3-12.* https://doi.org/10.26640/22159045.428

Moreno, M.; Baéz, L. (2021). Expedición Seaflower: El paisaje cultural marítimo de Providencia y Santa Catalina. Resultados preliminares. *Bol. Cient. CIOH, 40: 83-90.* https://doi.org/10.26640/22159045.2021.566

Nystuen, J.; Andrade, C. (1993). Tracking Mesoscale Ocean features in the Caribbean Sea using geosat altimetry. *Journal of Geophysical Reserch,* 98(C5): 8389-8394. https://doi.org/10.1029/93JC00125

Orejarena, A.; Restrepo, J.C.; Correa, A.; Orfila, A. (2022). Wave energy flux in the Caribbean Sea: Trends and variability. *Renewable Energy, 181: 616-629.* https://doi.org/10.1016/j.renene.2021.09.081

Ortega, S.; Osorio, A.; Agudelo, P. (2013). Estimation of the wave power resource in the Caribbean Sea in areas with scarce instrumentation Case study: Isla Fuerte, Colombia. *Renewable Energy, 57: 240-248.* https://doi.org/10.1016/j.renene.2012.11.038

Osorio, A.; Mesa, J.; Bernal, G.; Montoya, R. (2009). Reconstrucción de cuarenta años de datos de oleaje en el mar Caribe colombiano empleando el modelo WWIII y diferentes fuentes de datos. *Bol. Cient. CIOH, 27: 37-56.* https://doi.org/10.26640/22159045.200

Poveda, G. (1998). *Retroalimentación dinámica entre el Fenómeno El Niño-Oscilación del Sur y la hidrología de Colombia.* https://repositorio.unal.edu.co/handle/unal/51284

Pujos, G.; Mesa, O. (1988). Hydrogeology of the Colombian Caribbean continental platform around the Dique Delta in the rainy season: Consequences on circulation. *Bulletin de L'Institut de Geologie du Bassin d'Aquitaine, 44: 97-107.*

Rodríguez-Abal, D. (2019). Estudio de áreas de implementación de sistemas undimotrices en la costa gallega. Universidad Politécnica de Cartagena. España.

Rueda, S. (2017). Medidas regionales de planeamiento espacial marino para mejorar la sostenibilidad del Área Marina Protegida de Seaflower en el mar Caribe colombiano. Bol. Cient. CIOH, 35: 41-62. https://doi.org/10.26640/22159045.431

Ruiz, G.; Mendoza, E.; Silva, R.; Posada, G.; Pérez, D.; Rivillas, G.; Escalante, E.; Ruiz, F. (2009). Caracterización del régimen de oleaje y viento de 1948-2007 en el litoral mexicano. *Ingeniería del Agua, 16(1): 51-64.* https://doi.org/10.4995/ia.2009.2944

Ruiz, M.; Bernal, G. (2009). Variabilidad estaciona e interanual del viento en los datos del reanálisis NCEP/NCAR en la cuenca Colombia, mar Caribe. *Avances en Recursos Hidráulicos, 20: 7-20.*

Rusu, L.; Guedes, C. (2012). Wave energy assessments in the Azores islands. *Renewable Energy, 45: 183-196.* https://doi.org/10.1016/j.renene.2012.02.027

Shadman, M.; Roldán, M.; Pierart, F.; Haim, P.; Alonso, R.; Silva, C.; Osorio, A.; Almonacid, N.; Carreras, G.; Maali, M.; Arango, S.; Rosas, M.; Pelissero, M.; Tula, R.; Estefen, S.; Lafoz, M.; Saavedra, O. (2023). A review of offshore renewable energy in South America: current status and future perspectives. *Sustainability, 15(2), 1740.* https://doi.org/10.3390/su15021740

Sosa, M.; Hernández, A. (2002). Variación del estado de mar al paso de las ondas tropicales por el mar Caribe. *Revista de Climatología, 2: 1-4.*

Thomas, Y.; Nicolae, A.; Durand, P.; Posada, B.; García, C.; Andrade, C. A. (2011). Altura significativa del oleaje en la cuenca colombiana del Caribe datos de altimetría radar. Bol. Cient. CIOH, 29: 27-45. https://doi.org/10.26640/22159045.227

Thomas, Y.; Nicolae, A.; Posada, B. (2012). Atlas climatológico del mar Caribe colombiano. Instituto de Investigaciones Marinas y Costeras (Invemar)- Convenio Especial de Cooperación Colciencias. Gobernación del Magdalena.

Torres, R.; Andrade, C. (2006). Potencial en Colombia para el aprovechamiento de la energía no convencional de los océanos. *Bol. Cient. CIOH, 24: 11-25.* https://doi.org/10.26640/22159045.145

Torres, R.; Lonin, S. (2007). Estudio del espectro de oleaje en el Caribe observado con boyas y su representación en el espectro JONSWAP. *Bol. Cient. CIOH, 25: 8-18.* https://doi.org/10.26640/22159045.158

Van Rijn, L. C. 1994*. Principles of fluid flow and surface waves in rivers, estuaries, seas, and oceans*. Aqua Publications, Delft, Holanda. 335 pp.

Vega, M. J.; Álvarez, O.; Restrepo, J. C.; Ortiz, J. C.; Otero, L. J. (2020). Interannual variability of wave climate in the Caribbean Sea. *Ocean Dynamics,* 70: 965-976. https://doi.org/10.1007/s10236-020-01377-1

Vergaray, J. (2008). *Generación eléctrica mediante el aprovechamiento del oleaje marítimo costero. Universidad de Chile.*

Vernette, G. (1985). La plataforme continentale Caraibe du Colombie (du débouché du Magdalena au golfe de Morrosquillo). Importance du diapiris meargileux sur la morphologie et la sedimentation. Bordeaux: These de doctorado etates Sciencies present a Universite de Bordeaux.

Vicinanza, D.; Constetabile, P.; Ferrante, V. (2013). Wave energy potential in the north - west of Sardinia (Italy). *Renewable Energy,* 50: 506-521. https://doi.org/10.1016/j.renene.2012.07.015

Wang, C.; Lee, S. (2007). Atlantic warm pool, Caribbean low-level jet, and their potential impact on Atlantic hurricanes. *Geophysical Research Letters,* 34(2): 412-422. https://doi.org/10.1029/2006GL028579